Instantaneous frequency measurement based on transversal microwave filters with high resolution

Jianji Dong (董建绩)*, Yuan Yu (于 源), Xinliang Zhang (张新亮), and Dexiu Huang (黄德修)

Wuhan National Laboratory for Optoelectronics, Huazhong University of Science and Technology, Wuhan 430074, China

**Corresponding author: jjdong@mail.hust.edu.cn*

Received October 13, 2010; accepted January 3, 2011; posted online April 11, 2011

We propose a novel photonic technique for microwave frequency measurement based on transversal microwave filters with high resolution. Two parallel microwave filters with sine and cosine frequency responses are obtained by cross gain modulation in a single semiconductor optical amplifier, which introduces two different frequency responses to achieve an amplitude comparison function. We also demonstrate a proof-of-concept experiment. The measurement error is less than ±0.04 GHz for the first band range of 0–3.45 GHz and less than ±0.03 GHz for the second band range of 3.45–5.8 GHz. Our scheme is found to be capable of being extended for larger frequency range measurements using a shorter fiber length.

OCIS codes: 120.4570, 060.5625, 320.7100, 250.5980.
doi: 10.3788/COL201109.051202.

Instantaneous frequency measurement (IFM) receivers are required to enable scanning, identification, and analysis of the microwave signal over a large frequency range with a high probability of interception for modern electronic warfare. However, conventional IFM receivers suffer from high weight, finite bandwidth, high power consumption, and vulnerability to electromagnetic interference (EMI)[1]. Therefore, photonic approaches to IFM are attracting significant interests due to the inherent advantages of photonics, such as large bandwidth, low loss, and immunity to EMI[2,3]. The main idea is to achieve an amplitude comparison function (ACF) between two different transfer functions relative to the microwave frequency. Normally, sine and cosine functions are a pair of promising candidates for transfer functions to achieve high-resolution ACF[4−9] because they have complementary characteristics, where one is a low pass filter and the other is a band pass filter. A very steep ACF can be obtained by contrasting these two functions. Generally, photonic IFM can be implemented using a photonic microwave filtering response. For instance, Zhou *et al.* presented an IFM with a large range using sine and cosine functions as transfer functions. A large frequency range was measured with the cost of large error estimation[10]. An infinite impulse response scheme was also presented by the same group. Since an electrical feedback loop was used, the small free spectral range (FSR) could make the measurement range rather small, with values only within tens of megahertzs[11]. Zou *et al.* presented an IFM method by dispersion induced microwave filter. Extremely high resolution was measured in high frequency while the measurement error was observed to be large in low frequency range[12].

Semiconductor optical amplifiers (SOAs) are widely used in nonlinear optical signal processing[13−15] and microwave photonic filters[16−20] due to their ultrafast dynamic response and low power consumption. In terms of microwave photonic filters, Coppinger *et al.* presented a negative coefficient transversal filter based on cross gain modulation (XGM), which demonstrated sine transfer functions[16]. Mora *et al.* presented photonic filters with arbitrary positive and negative coefficients based on SOAs[17]. Sarkhosh *et al.* presented an IFM approach by nonlinear optical mixing in a SOA[21]. Thus, a variety of transfer functions can be easily obtained using the nonlinearities of SOAs.

In this letter, we propose a photonic approach to IFM based on transversal microwave filters using XGM effect in a single SOA. Different from Refs. [11, 17], we employ the differential group delay induced by the dispersion of single-mode fiber (SMF) instead of the optical delay line to achieve larger FSR. Hence, a large frequency measurement range can be obtained for the IFM system. Compared with Refs. [10–12], our scheme shows a significantly higher measurement resolution. A frequency band from 3.45 to 5.8 GHz with a measurement error less than ±0.03 GHz and another frequency band from 0 to 3.45 GHz with a measurement error less than ±0.04 GHz are demonstrated.

The operation principle of the IFM system is described in Fig. 1. The first laser diode (LD1) emits a continuous wave (CW) at wavelength λ_1, which is modulated by a Mach-Zehnder modulator (MZM), driven by an unknown radio-frequency (RF) signal. The modulated optical signal and three other CW beams (λ_2, λ_3, and λ_4) are introduced into a nonlinear SOA (CIP Technologies) to arouse the XGM effect. These three CW beams are modulated with inverted information to the original tap. Consequently, a fiber Bragg grating (FBG) serves as a wavelength de-multiplexer. The upper two beams (λ_1, λ_2) will yield output from the transmission port of the FBG, and the lower two beams (λ_3, λ_4) will produce output via the reflection port of the FBG. Two sections of SMFs are used to introduce a certain time delay between the two taps of the microwave filters, respectively. The upper microwave filter reveals a sine transfer function because the two taps are out of phase. However, the lower filter exhibits a cosine transfer function because the two taps are in phase. Finally, the microwave powers of the two parts are measured by two photodetectors (PDs), and a fixed frequency-to-power mapping is established in the post processing.

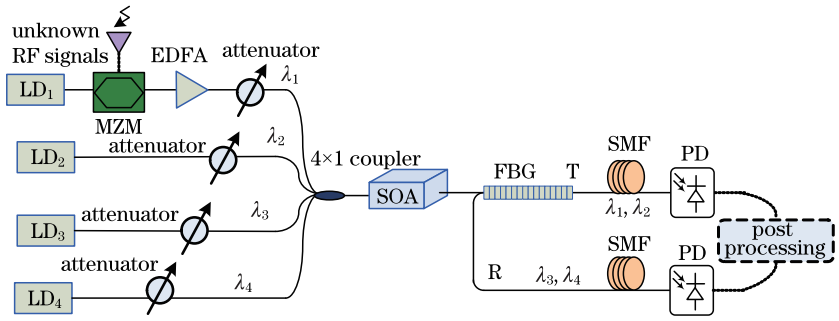

Fig. 1. Schematic diagram of the proposed IFM system. EDFA: erbium-doped fiber amplifier; T: transmission port; R: reflection port.

Assuming that the two taps of the transversal filter have the same amplitude, then the tap coefficients for the lower filter and the upper filter are [1, 1] and [1, –1], respectively. Therefore, the RF powers at the outputs of the two PDs are

$$H_1(f) = R_1 \cos^2(\pi f \tau_1), \tag{1}$$

$$H_2(f) = R_2 \sin^2(\pi f \tau_2), \tag{2}$$

where f is the frequency of the unknown microwave signal, and τ_i (i=1, 2) are the time delay differences between the two taps. This can be expressed as $\tau_i = Dl\delta\lambda_i$, where D and l are dispersion parameter and fiber length, respectively, and $\delta\lambda_i$ is the wavelength span. R_i (i=1, 2) are the total losses of the two arms, including the insertion loss of the coupler, modulator, FBG, SMF, and the responsivity of the PDs. Through calibration and post-processing, $R_1 = R_2$ can be obtained. Thus, the ACF can be expressed by

$$\mathrm{ACF}(f) = \frac{H_1(f)}{H_2(f)} = \frac{\cos^2(\pi f \tau_1)}{\sin^2(\pi f \tau_2)}. \tag{3}$$

Using Eq. (3), the RF frequency can be calculated from the measured ACF.

Figure 2 simulates the frequency responses of the two transversal filters and the resultant ACF, where τ_1=144 ps and τ_2=171 ps. The transfer function $H_1(f)$ monotonously decreases, while the transfer function $H_2(f)$ monotonously increases from 0 GHz to the first notch of the frequency. Therefore, the ACF exhibits a steep frequency-to-power mapping, resulting in a high resolution or accuracy. The upper limit of the measurement range, f_{up}, is determined by the first notch position of the transfer function, where $f_{\mathrm{up}} = \frac{1}{2\tau_1}$.

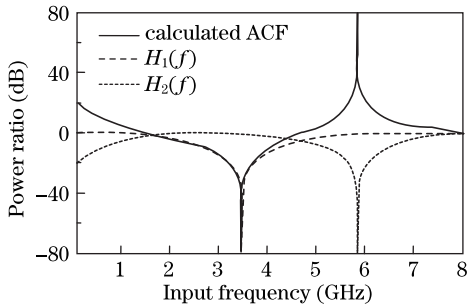

Fig. 2. Simulated transfer functions and resultant ACF.

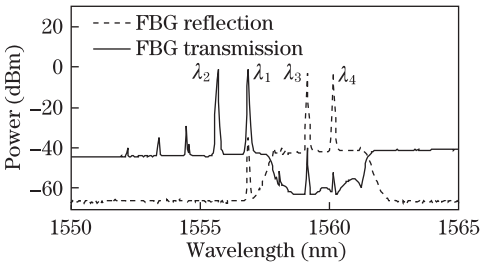

Fig. 3. Reflection and transmission spectra of the FBG when four LDs are launched into the SOA simultaneously.

A proof-of-concept experiment was performed, as shown in Fig. 1. Frequency responses of the two-tap transversal microwave filters were measured by connecting the input and output ports of a vector network analyzer (Anritsu 37369D) to the PD and the MZM, respectively. Emitted wavelengths from the four LDs, λ_1, λ_2, λ_3, and λ_4, were 1556.87, 1555.67, 1559.15, and 1560.15 nm, respectively. The MZM has a response bandwidth of 10 GHz. The attenuators (ATTs) before the SOA were used to control the input power of each tap. The bias current for the SOA was 240 mA. Length and dispersion parameters of the SMF were 20 km and 7.1 ps/(nm· km), respectively. Therefore, time delays for the two taps were τ_1=144 ps and τ_2=171 ps.

Figure 3 shows the reflection and transmission spectra of the FBG when four LDs are launched into the SOA simultaneously. Four beams are split into two routes, and in each route, the powers of the two taps are almost equal; thus, the tap coefficients are [1, 1] and [1, –1] for the two transversal filters.

The measured ACF and the transfer functions for the two transversal filters are shown in Fig. 4. The measured ACF agrees well with the calculated ACF with a notch at 3.45 GHz. Based on Eq. (3), a look-up table is set up and the microwave frequency is estimated using the measured ACF. Figures 5(a) and (b) show the comparison between the measured and theoretical frequencies and measurement errors, respectively. If the frequency upper limit terminates at the first notch of transfer functions, the measurement range is 0–3.45 GHz (Band 1) with the measurement error of ±0.04 GHz. At the same time, a more discernible power variation from 3.45–5.8 GHz is evident, defined as Band 2. The steep ACF reveals a higher measurement resolution. In Fig. 5(b), the frequency error is less than ±0.03 GHz.

Although the experiment results demonstrate a maximum measured frequency of 5.8 GHz only, the

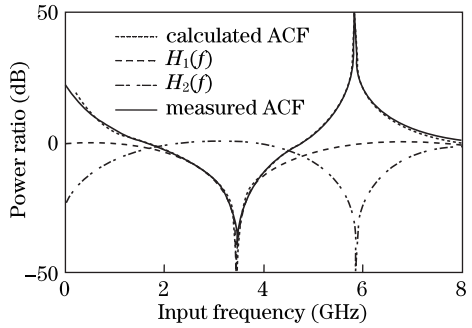

Fig. 4. Transfer functions for two transversal filters and corresponding ACF.

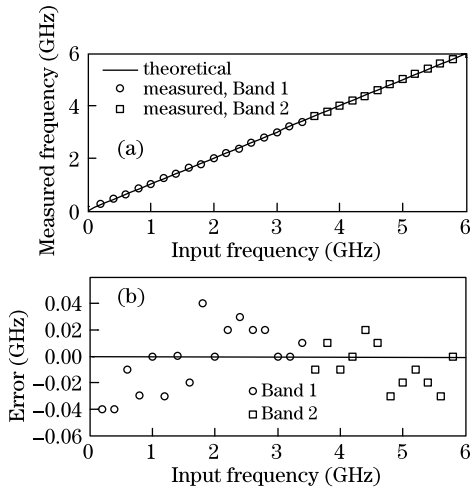

Fig. 5. (a) Measured frequency versus input frequency, (b) measurement errors. Different frequency bands are measured for comparison.

measurement range can be extended further. A large frequency range can be measured using a shorter SMF length to introduce a smaller time delay. Furthermore, the frequency measurement range is limited only by the bandwidth of the MZM. On the other hand, there is a trade-off between the measurement range and the measurement accuracy. Less measurement errors result from a narrow measurement range. Therefore, the measurement error will be extended for a larger band measurement.

In conclusion, we propose a novel photonic approach to IFM based on transversal microwave photonic filters, which produce frequency responses with sine and cosine functions. For the first frequency band range of 0–3.45 GHz, the measurement error is less than ±0.04 GHz; while for the second band range of 3.45–5.8 GHz, the measurement error is less than ±0.03 GHz. Compared with the optical delay line between different taps, the SMF can produce a negligible time delay in order to obtain a large frequency measurement range. The measurement range can be extended further using a shorter fiber length, and the maximum frequency measurement is limited only by the bandwidth of MZM.

This work was supported by the National Basic Research Program of China (No. 2006CB302805), the National Natural Science Foundation of China (No. 60901006), and the Program for New Century Excellent Talents of the Ministry of Education of China (No. NCET-04-0715).

References

1. M. Aikawa and H. Ogawa, IEEE Trans. Microwave Theor. Tech. **37,** 406 (1989).
2. J. Capmany and D. Novak, Nature Photon. **1,** 319 (2007).
3. J. Yao, J. Lightwave Technol. **27,** 314 (2009).
4. J. Dai, K. Xu, X. Sun, J. Niu, Q. Lv, J. Wu, X. Hong, W. Li, and J. Lin, IEEE Photon. Technol. Lett. **22,** 1162 (2010).
5. J. Li, S. Fu, K. Xu, J. Q. Zhou, P. Shum, J. Wu, and J. Lin, Opt. Lett. **34,** 743 (2009).
6. M. V. Drummond, P. Monteiro, and R. N. Nogueira, Opt. Express **17,** 5433 (2009).
7. J. Zhou, S. Fu, S. Aditya, P. P. Shum, and C. Lin, IEEE Photon. Technol. Lett. **21,** 1069 (2009).
8. H. Chi, X. Zou, and J. Yao, IEEE Photon. Technol. Lett. **20,** 1249 (2008).
9. X. Zou, H. Chi, and J. Yao, IEEE Trans. Microwave Theor. Tech. **57,** 505 (2009).
10. J. Zhou, S. Fu, P. P. Shum, S. Aditya, L. Xia, J. Li, X. Sun, and K. Xu, Opt. Express **17,** 7217 (2009).
11. J. Zhou, S. Aditya, P. P. Shum, and J. Yao, IEEE Photon. Technol. Lett. **22,** 682 (2010).
12. X. Zou, W. Pan, B. Luo, and L. Yan, IEEE Photon. Technol. Lett. **22,** 1090 (2010).
13. J.-J. Dong, X.-L. Zhang, and D.-X. Huang, Chin. Phys. B **17,** 4226 (2008).
14. J. Dong, X. Zhang, J. Xu, D. Huang, S. Fu, and P. Shum, Opt. Lett. **32,** 1223 (2007).
15. J.-J. Dong, X.-L. Zhang, and D.-X. Huang, Chin. Phys. Lett. **24,** 3450 (2007).
16. F. Coppinger, S. Yegnanarayanan, P. D. Trinh, and B. Jalali, Electron. Lett. **33,** 973 (1997).
17. J. Mora, A. Martinez, M. D. Manzanedo, J. Capmany, B. Ortega, and D. Pastor, Electron. Lett. **41,** 921 (2005).
18. Y. Xiaoke, F. Wei, N. J. Hong, and L. Chao, IEEE Photon. Technol. Lett. **13,** 857 (2001).
19. N. You and R. A. Minasian, J. Lightwave Technol. **24,** 2558 (2006).
20. E. Xu, X. Zhang, L. Zhou, Y. Zhang, Y. Yu, X. Li, and D. Huang, Opt. Lett. **35,** 1242 (2010).
21. N. Sarkhosh, H. Emami, L. Bui, and A. Mitchell, in *Proceedings of 2008 IEEE MTT-S International Microwave Symposium Digest* 599 (2008).